

# Using Interferometry to Determine the Wavelength of HeNe Laser and the Indices of Refraction of Air and Helium

Gonghan Xu

A Michelson interferometer was used to investigate the wavelength of HeNe laser and the indices of refraction of air and helium at normal room conditions. The wavelength of HeNe laser was determined to be 683.0nm. The index of refraction of air was determined to be 1.0002184. The index of refraction of helium was determined to be 1.00007302 and 1.00004700 in two separate groups of experiments. These results do not align with the published values perfectly, but the deviations are reasonable given the experimental conditions.

## 1 Introduction

In 1801, Thomas Young showed that two overlapping light waves can interfere with each other in his famous double-split experiment. Using the interference pattern of candle light, he was able to determine the wavelength of light for the first time in history.<sup>1</sup> This established the basis of interferometry - techniques that utilize the interference phenomenon of light to obtain useful information, and interferometers - devices that operate based on interferometry.<sup>2</sup>

Interferometry has applications in a wide range of fields. Probably the most famous application (and one of the earliest) is the Michelson-Morley experiment that disproved the existence of ethers in 1887.<sup>2</sup> In radio astronomy, Martin Ryle applied interferometry to radio telescopes in the 1960s so that multiple telescopes could collaborate with each other to resolve images to an extent that would require a single telescope of a much larger diameter.<sup>2</sup> In medicine, interferometry has been used in optical coherence tomography (OCT) to obtain cross-sectional images of internal structures of biological tissues noninvasively.<sup>3</sup> In seismology (the study of earthquakes), seismic interferometry is starting to reveal useful information from complicated Earth signals that were previously regarded as background noise.<sup>4</sup> A more recent triumph of interferometry occurred in 2015 when LIGO (The Laser Interferometer Gravitational-Wave Observatory) detected gravitational waves for the first time. LIGO detected the gravitational wave signal using two modified Michelson interferometers, each having two orthogonal arms 4km long.<sup>5</sup>

In general, interferometry is a very useful technique to measure extremely small distances and displacements.<sup>2</sup> To demonstrate this, interferometry-related experiments are often carried out in undergraduate laboratories today. As an undergraduate student, I used a Michelson interferometer to measure the wavelength of HeNe laser and the indices of refraction of air and helium at normal room conditions.

## 2 Theory

The primary theoretical concern in this experiment is the interference phenomenon of light. In general, when two coherent waves (i.e. constant phase difference) of the same nature arrive at the same point in phase (i.e. crest-to-crest and trough-to-trough), their amplitudes will add up and the resulting superimposed wave will have a larger amplitude. This is called a constructive interference. When the two coherent waves arrive at the same point out of phase (i.e. crest-to-trough and trough-to-crest), their amplitudes will subtract each other, hence a destructive interference. When the two coherent waves arrive at the same point neither in phase nor out of phase, the resulting total amplitude will be between those of constructive and destructive interferences.<sup>6</sup>

The interference phenomenon can be visualized with the fringe pattern in Young's double slit experiment. As shown in Figure 1, two monochromatic, in-phase light sources at the closely-spaced, narrow slits  $S_1$  and

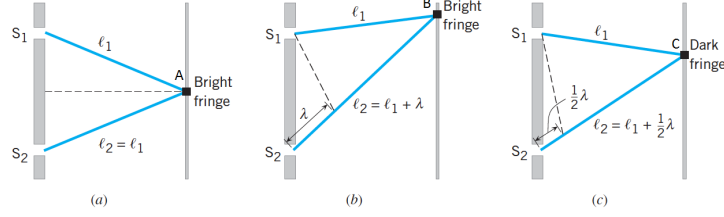


Figure 1: Interference of light in the double slit experiment

$S_2$  will produce an image on a projection board parallel to and far away from the slits. Due to the ability of light to diffract, which means that light can bend around obstacles or edges of an opening,<sup>7</sup> light beams emitted from the two sources can reach different positions on the projection board.

As shown in Figure 1(a), at Point A, two light beams from  $S_1$  and  $S_2$  will interfere constructively since they have travelled the same distance to reach this point and are thus still in phase. Therefore, the intensity of light at Point A will be twice the intensity if there were only a single light beam, and thus a bright fringe can be seen at this point. In Figure 1(b), a light beam from  $S_2$  has traveled an additional distance of a wavelength than a beam from  $S_1$  when they reach Point B simultaneously. Since the two light beams now have a phase difference of one wavelength, they are indeed still in phase and will interfere constructively at this point. Therefore, another bright fringe will show at Point B. Similarly, when a light beam from  $S_1$  travels an additional wavelength than one from  $S_2$ , a bright fringe will form symmetrically at the other side of Point A (not shown in Figure 1(b)). In general, if a light beam travels an additional integer number of wavelengths than another light beam when they simultaneously arrive at the same point, then there will be a constructive interference of the two light waves at that point. As per Figure 1(c), a dark fringe will form at Point C between Point A and Point B. This is because a light beam from  $S_2$  has travelled an additional half wavelength than that from  $S_1$  to reach Point C and hence they interfere destructively at this Point. In general, if a light beam travels an additional odd number of half wavelengths than another light beam when they simultaneously arrive at the same point, then there will be a destructive interference of the two light waves at that point. Therefore, there will be an alternating bright and dark fringes pattern on the projection board with a symmetric layout with respect to the central bright fringe at Point A.<sup>1</sup>

Another theoretic concern for this experiment is the linear relation between the index of refraction (or called refractive index) of a gas and its pressure at constant temperature. For most dielectric materials, the material's index of refraction  $n$  can be approximated by  $\sqrt{\epsilon_r}$ , where  $\epsilon_r$  is the material's dielectric constant. When electromagnetic waves (light) propagate through such a dielectric medium, electrons in the atoms and molecules of the dielectric medium will experience an oscillating electric field and will thus oscillate around their original positions (we neglect the oscillations of the much more massive and hence much less mobile nuclei). The oscillating electrons will produce oscillating dipole moments and thus a total polarization of the dielectric medium. The dielectric constant  $\epsilon_r$ , and hence the index of refraction, will depend on how the dielectric material polarizes under the applied electric field (the propagating light). In the case of a dilute gas and a propagating monochromatic light, we can establish a proportional relationship between  $n-1$  and the total number density  $\sigma$  of atoms and molecules of the dilute gas:

$$n - 1 = A\sigma \quad (1)$$

where  $\sigma$  is the total number density of the atoms and molecules in the gas, and  $A$  is a proportionality constant.<sup>8</sup> For an ideal gas, the number density of the gas molecules and atoms is proportional to  $\frac{P}{T}$ , where  $P$  is the gas pressure and  $T$  is the gas temperature. Therefore, for a dilute gas with constant temperature, we can establish the following relationship:

$$n = kP + 1 \quad (2)$$

where  $k$  is a proportionality constant (I will call  $k$  the linear coefficient in this document). If we consider the influence of the change of pressure on the change of index of refraction for the dilute gas at constant

temperature, we have

$$\frac{\Delta n}{\Delta P} = k \quad (3)$$

### 3 Experiment

#### 3.1 General experimental setup

As shown in Figure 2, this experiment was carried out on an Michelson interferometer built on an optical bread board placed horizontally on a table. In the following detailed discussion of these optical apparatus and the experimental theories, I will use directional terms, such as “horizontal”, “vertical”, “left”, “right”, “up”, and “down”, with respect to Figure 2 rather than the real experimental environment.

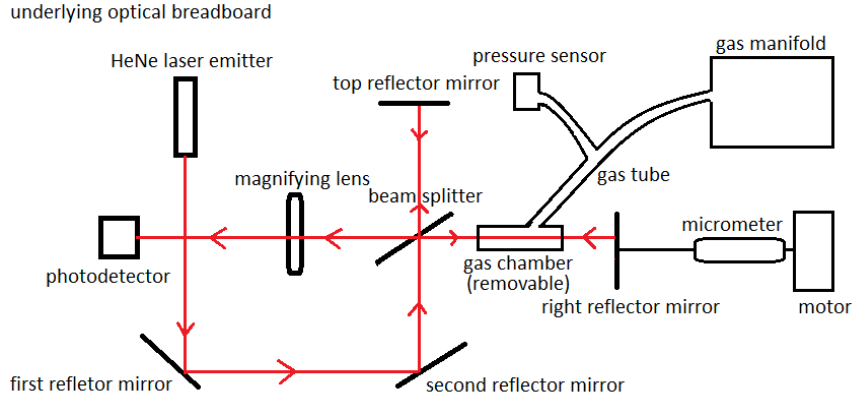


Figure 2: Setup of the interferometry experiment

As shown in Figure 2, A beam of HeNe laser of wavelength 632.8nm in air is emitted from a laser emitter and impinges on the the first reflector mirror oriented 135 degrees to the horizontal direction. The reflected laser will hit the second reflector mirror, oriented 45 degrees to the horizontal direction, and be reflected again onto the beam splitter. The beam splitter is also aligned 45 degrees to the horizontal direction so that the incoming laser is split into two separate beams, one going up toward the top reflector mirror and the other going right toward the right reflector mirror. The top reflector mirror and the right reflector mirror will reflect incidence beams back to the beam splitter. Part of the beam reflected from the top reflector mirror will be reflected by the beam splitter toward the photodetector on the left, while part of the beam reflected by the right reflector mirror will go through the beam splitter and also head toward the photodetector. (At the beam splitter, the other part of the reflected beams from the top and the right reflector mirrors will return to the laser source along their original travelling route and thus are not interesting to us.) Between the photodetector and the beam splitter is a convex lens, which magnifies the image of the impinging light on the photodetector so that the interference pattern of the two converging light beams are more clearly visible. The photodetector can detect the intensity of the incoming light, which can be recorded by a computer interface on a computer connecting to the photodetector.

As shown in Figure 2, the horizontal position of the right reflector mirror is adjustable (while keeping the reflector mirror’s orientation unchanged) by a micrometer of a measuring range of 0-2.5mm. The driving screw of the micrometer can be attached to a motor that rotates one revolution per minute, corresponding to a 0.05mm horizontal displacement of the right reflector mirror to the right. Besides, a gas chamber of internal chamber length of 100mm can be placed horizontally between the beam splitter and the right reflector mirror. The gas chamber is connected to a gas manifold through a gas tube. As shown in Figure 3, the gas tube coming from the gas chamber is branched into multiple pipes on the gas manifold. The opening and closing of these pipes can be controlled with valves along pipe ways. Only two pipe ways on the gas manifold are of interest to us. One of them (the gas inlet pipe) is connected to a syringe barrel without a plunger, and the other (the gas pumping pipe) is connected to a vacuum pump. When the valve on the gas

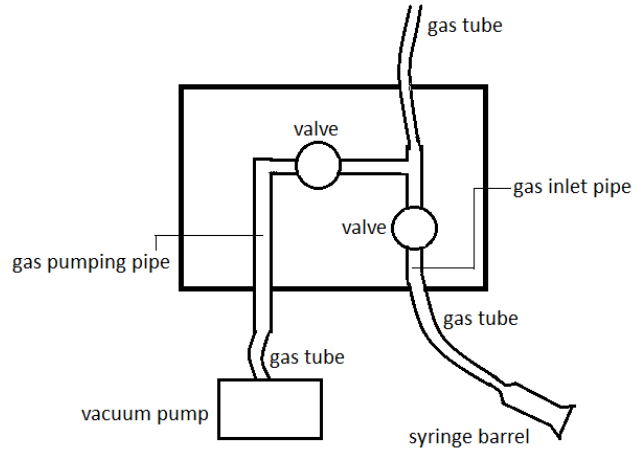


Figure 3: The gas manifold

pumping pipe is sealed and that on the gas inlet pipe is on, air (or any other kind of gas) on the outer end of the syringe barrel can flow into the gas inlet pipe and then into the gas chamber through the gas tube. When the valve on the gas inlet pipe is closed and that on the gas pumping pipe is open, the vacuum pump connected to the gas pumping pipe can be turned on to draw gas out of the gas chamber. The valve on the gas pumping pipe can then be closed after all of the gas in the gas chamber are drawn out so that the gas chamber is left in vacuum. As shown in Figure 2, the gas tube connecting the gas manifold and the gas chamber is branched out mid-way to a pressure sensor. Therefore, when the gas in the gas chamber settles into equilibrium, its pressure can be measured by the pressure sensor. The pressure sensor is connected to the same computer interface as the photodetector is and thus its readings can be recorded simultaneously with those of the photodetector.

## 3.2 Determining the wavelength of HeNe laser

### 3.2.1 Experimental theory

As shown in Figure 2, when the horizontal distance between the beam splitter and the right reflector mirror increases, the light beam that is horizontally-split at the beam splitter will ultimately travel back to the beam splitter and have travelled an additional distance twice that travelled by the right reflector mirror. Let the displacement distance of the right reflector mirror be  $\Delta d$ , and the wavelength of the HeNe laser in air be  $\lambda_{air}$ . Then the additional number of wavelengths that the horizontally-split beam will travel before returning to the beam splitter is  $\Delta N = \frac{2\Delta d}{\lambda_{air}}$ . As mentioned in Section 2, When  $\Delta N$  is an integer, the interference patterns of the light image on the photodetector will be the same because the phase differences between the arriving light beams on the photodetector are indeed the same. So, if we can record the instantaneous intensities of the converging light beams and the corresponding times as the right reflector mirror moves to the right at a constant speed, we can find out the time intervals between successive constructive interferences by locating the local maximum intensities. These successive peak intensities correspond to successive increases of the number of wavelengths travelled by the horizontally-split beam. Take one such time interval to be  $\Delta t$ , and the speed of the right reflector mirror to be  $v$ . Then during this time interval  $\Delta t$ , the right reflector mirror has travelled an additional distance of  $v\Delta t$ , and therefore the horizontally-split light beam will have travelled an additional distance of  $2v\Delta t$  before it returns to the beam splitter. Then ideally, we should have

$$\lambda_{air} = 2v\Delta t \quad (4)$$

We can measure the intensity of light on the photodetector for a period to obtain a number of such time intervals in a consecutive order. With Equation 4 and these consecutive time intervals, an average value for the HeNe laser wavelength can be found using linear line fitting.

### 3.2.2 Procedure

For this experiment, the gas chamber was not used, so there was only air between the beam splitter and the right reflector mirror. The room air temperature was taken to be about 23 °C as the typical temperature for the laboratory. The outdoor air pressure and humidity was taken from the weather report to be about 1.0030atm and about 37 percent, respectively. These outdoor parameters will be used to approximate the room air conditions.

First, the HeNe laser emitter was turned on. Then, the positions and orientations of the reflector mirrors and the photodetector were adjusted so that the impinging light fell right on the photodetector and showed an obvious interference pattern with a relatively wide central fringe. To ascertain interference happened on the photodetector, the horizontal position of the right reflector mirror was adjusted with the micrometer by hand to see the fringes moving on the photodetector. The driving screw of the micrometer was then turned nearly to the one end so that the micrometer could be driven by the motor without hitting the other end for a sufficient amount of time. After this, the motor was attached to the micrometer and turned on to displace the right reflector mirror horizontally to the right. Then the computer interface was turned on to record the instantaneous intensities of the impinging light on the photodetector very 0.001 second for 30 seconds.

## 3.3 Determining indices of refraction of air and helium

### 3.3.1 Experimental theory

When a gas chamber filled with some amount of gas is placed between the beam splitter and the right reflector mirror, the horizontally-split laser will need to travel through the gas chamber twice before it returns back to the beam splitter. When the gas in the gas chamber has a different index of refraction from that of the air in the room, the wavelength of the light beam in the gas chamber will be different from that of the same light beam outside the gas chamber (i.e. in the surrounding air). Let the index of refraction of the gas in the gas chamber be  $n_c$ , then the wavelength of the HeNe laser in the gas chamber will be  $\frac{\lambda_0}{n_c}$ , where  $\lambda_0$  is the wavelength of the HeNe laser in vacuum. Supposing the internal length of the gas chamber is  $l$  and the number of wavelengths in the gas chamber when the light beam propagates through is  $M$ , then we have

$$M = \frac{l}{\lambda_0/n_c} = \left(\frac{l}{\lambda_0}\right)n_c \quad (5)$$

So, the larger the index of refraction of the gas in the gas chamber, the more wavelengths the gas chamber will be able to accommodate. Suppose the index of refraction of the gas in the gas chamber is initially  $n_1$  and changes to  $n_2$  afterwards. Then the horizontally-split beam will travel an additional  $\Delta N = 2(M_2 - M_1)$  number of wavelengths during its trip from the beam splitter to the right reflector mirror and then back to the beam splitter ( $M_1$  and  $M_2$  are the number of wavelengths in the gas chamber initially and afterwards, respectively). According to Equation 5, we then have

$$\Delta N = 2(M_2 - M_1) = \left(\frac{2l}{\lambda_0}\right)(n_{c2} - n_{c1}) = \left(\frac{2l}{\lambda_0}\right)\Delta n \quad (6)$$

where  $\Delta n$  is the change of index of refraction of the gas in the gas chamber. Then we have

$$\Delta n = \left(\frac{\lambda_0}{2l}\right)\Delta N \quad (7)$$

Since we know  $\lambda_0$ , which is the wavelength of the HeNe laser in vacuum, and  $l$ , which is the internal length of the gas chamber, as long as we know twice the change of the wavelength capacity of the gas chamber ( $\Delta N$ ) between Instant 1 ( $M = M_1$ ) and Instant 2 ( $M = M_2$ ), we can know the corresponding change of refractive index of the gas in the gas chamber between Instant 1 and Instant 2 ( $\Delta n$ ).

According to Section 2, at constant temperature the change of index of refraction of the gas in the gas chamber (both air and helium at normal room conditions are dilute) is proportional to the change of its pressure. So if we increase the pressure of the gas in the gas chamber continuously by pumping in the same kind of gas, the index of refraction of the gas chamber gas should also increase continuously. As per Equation 5, this means that the total number of wavelengths that the gas chamber can accommodate will

also increase continuously. Let's consider the two instants when  $M = M_1$  and  $M = M_2$  again. Since the time it takes for light to travel through one wavelength is always the same as long as its frequency stays unchanged, if  $\Delta N = 2(M_2 - M_1)$  is an integer (remember that the horizontally-split beam travels in a round trip), the interference pattern of the converged light beams on the photodetector will be the same for Instant 1 and Instant 2. As a result, the converging light beams at the photodetector will change and repeat their interference pattern continuously, such that the central fringe will change from bright to dark and from dark to bright, and so on and so forth. This phenomenon will be displayed on the computer interface as a semi-periodic fluctuation of the detected light intensity. This mechanism is essentially the same as that to let the horizontally-split beam travel additional wavelengths in the wavelength experiment (the experiment to determine the wavelength of HeNe laser) described in Section 3.2.1. In the wavelength experiment we increased the number of wavelengths travelled by the horizontally-split beam by increasing its travelling distance, while in this experiment we achieve the same effect by shrinking the wavelength of the horizontally-split beam along a portion of its travelling route. So, like in the wavelength experiment, the additional number of wavelengths  $\Delta N$  travelled by the horizontally-split beam can be read off from the computer interface directly by counting successive peaks of intensity. Since the computer interface records the gas pressure at the same time, we can read off the corresponding pressure increases  $\Delta P$ . According to Equation 3 and Equation 7, we have

$$k = \left(\frac{\lambda_0}{2l}\right)\left(\frac{\Delta N}{\Delta P}\right) \quad (8)$$

So, data collected by the photodetector and the pressure sensor when the gas is being pumped into the gas chamber can be used to calculate the linear coefficient  $k$  of the gas.

### 3.3.2 Procedure

Since the recorded pressures of the gas chamber gas were only on a relative scale on the computer interface, the pressure reading when the gas chamber was maintained in vacuum and that when the gas chamber was open to the room environment were recorded so that all pressure readings could be calibrated to absolute pressure values. The room air temperature was taken to be 23 °C and the outdoor air pressure and humidity were taken from the weather report to be about 1.0103atm and 40 percent, respectively. Like in the wavelength experiment, these outdoor parameters will be used to approximate the laboratory condition. Initially, all of the valves on the gas manifold were closed, and the syringe at the end of the gas inlet pipe was open to air in the laboratory. Two sets of experiments were conducted, one to measure the index of refraction of air and the other to measure the index of refraction of helium.

For the first set of experiments (Set 1), 6 trials were carried out. For each trial, like in the wavelength experiment, the HeNe laser emitter was turned on and the light beams were made to converge on the photodetector with an obvious interference pattern and a wide central fringe. The gas chamber was initially set to a state of vacuum with the vacuum pump. Then the valve on the gas pumping pipe was closed and that on the gas inlet pipe was opened to let air flow into the gas chamber. During the period between when air started to enter the gas chamber and when the detected pressure of the gas chamber air stopped increasing, the intensities of the interfering light beams and the pressures of the gas chamber air, along with the corresponding times, were recorded by the computer interface 1000 times per second for 5 seconds. For each trial, I tried to record the data at different pressure ranges of the air in the gas chamber.

The other set of experiments (Set 2) consists of 2 groups of trials. The first group (Set 2 Group 1) is comprised of 6 trials of experiments, while the second group (Set 2 Group 2) includes 4 trials. All 10 trials of experiments in Set 2 were conducted the same way as the trials of Set 1 except that helium instead of air was used to fill the gas chamber. This was realized by sealing the outer end of the syringe barrel to a bag of helium gas with scotch tape. Besides, for the first group of 6 trials in Set 2, the gas inlet valve was opened to a smaller extent than it was for the second group of 4 trials so that helium was expected to flow into the gas chamber faster in the second group of trials. Moreover, Set 2 Group 2 Trial 1 was conducted with a data recording period of 5 seconds, while all the other 3 trials in the same group were carried out with a data recording period of 10 seconds.

To minimize pollution of the content in the gas chamber, before Set 2 was carried out, a purging process was executed with the vacuum pump. First, the helium bag was sealed to the syringe barrel with the valve on the gas inlet pipe closed. Then, the vacuum pump and the gas pumping valve were turned on to remove

the remaining air in the gas chamber. After the remaining air was removed (this was indicated by the pressure reading on the computer interface), the gas pumping valve was closed (while leaving the vacuum pump running) and the gas inlet valve was opened to let helium from the helium bag enter and fill up the gas chamber. After the gas chamber helium pressure stopped increasing, the gas inlet valve was closed again and the gas pumping valve was opened again to purge the gas in the gas chamber. This process was repeated several times to ensure that most of the remaining air in the gas chamber, the gas tube, and the gas manifold pipes from Set 1 was removed.

## 4 Data analysis

### 4.1 Determining the wavelength of HeNe laser

As described in Section 3.2.2, for the experiment to determine the wavelength of HeNe laser in the laboratory environment, the intensities of the interfering light beams on the photodetector along with their respective times were recorded on the computer interface every 0.001 second for 30 seconds. A computer program was written to pinpoint the maximum intensities (corresponding to constructive interferences) of the data set, and 76 maximum intensities were identified. According to Equation 4, we care about only the time intervals between successive maximum intensities. As shown in Figure 4, in order to get an average of these

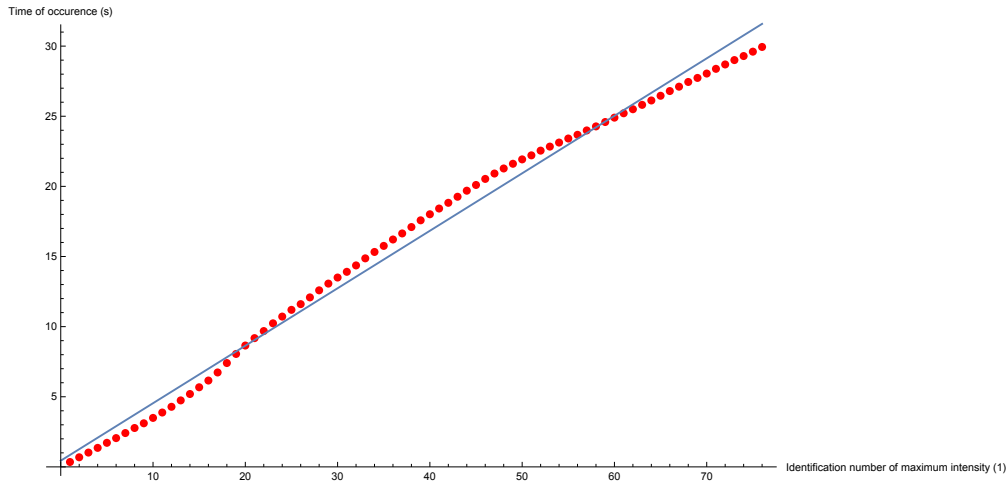


Figure 4: The wavelength experiment: times of occurrence of constructive interferences

time intervals, I used a line  $t = aN + b$ , where  $t$  is the time of occurrence of a maximum intensity and  $N$  is the maximum intensity's identification number, to fit the maximum intensities data points. The fitting result from Mathematica is  $t = 0.409788N + 0.441802$ , so the average time interval  $\Delta t$  between two consecutive maximum intensities is 0.409788 seconds. Recall from Section 3.1 that the displacement speed of the right reflector mirror was  $v = 0.05\text{mm}/\text{min} = 833.3\text{nm}/\text{s}$ . So, from Equation 4, we can determine the wavelength of the HeNe laser in the laboratory setting to be  $\lambda_{air} = 2v\Delta t = 2 \times 833.3\text{nm}/\text{s} \times 0.409788\text{s} = 683.0\text{nm}$ . Recall from Section 3.1 that the HeNe laser wavelength in air should be around 632.8nm, so the experimentally determined wavelength is larger than the expected wavelength by about 8 percent.

### 4.2 Determining indices of refraction of air and helium

#### 4.2.1 Index of refraction of air

As mentioned in Section 3.3.2, to determine the index of refraction of air at room temperature, 6 trials were carried out. Table 1 documents the gas chamber air pressures and the corresponding times at constructive interferences of the interfering light beams. Notice that I use rap, which stands for room air pressure, as a unit for pressure in Table 1 because the recorded pressures on the computer interface are the most

Air Trial 1		Air Trial 2		Air Trial 3	
time(s)	pressure(rap)	time(s)	pressure(rap)	time(s)	pressure(rap)
0.325	0.456980228	0.3	0.267405632	0.35	0.566986219
0.725	0.470437388	0.74	0.284373877	0.95	0.583954464
1.175	0.485068904	1.06	0.296656681	1.45	0.597998802
1.625	0.499700419	1.46	0.311875374	1.95	0.611455962
2.075	0.513732774	1.86	0.327082085	2.45	0.624913122
2.575	0.529538646	2.18	0.338789694	3.05	0.639544638
2.975	0.54182145	2.62	0.355170761	3.65	0.654751348
3.425	0.554691432	2.98	0.368040743	4.25	0.669382864
3.975	0.571659676	3.38	0.382672259	4.85	0.682840024
4.475	0.58512882	3.78	0.396716597		
		4.22	0.411923307		
		4.62	0.425967645		
Air Trial 4		Air Trial 5		Air Trial 6	
time(s)	pressure(rap)	time(s)	pressure(rap)	time(s)	pressure(rap)
0.187	0.467513481	0.55	0.765919712	0.85	0.761833433
0.637	0.482144997	1.45	0.781138406	1.65	0.775290593
1.087	0.496189335	2.25	0.79342121	2.55	0.789910126
1.537	0.510808868	3.15	0.80687837	3.45	0.803954464
1.987	0.524853206	4.05	0.819760336	4.45	0.81858598
2.437	0.538897543				
2.962	0.554116237				
3.412	0.566986219				
3.862	0.579856201				
4.387	0.595074895				

Table 1: Gas chamber air pressures at constructive interferences. The unit, rap, means room air pressure.

easily scaled with respect to the room air pressure. Therefore, a pressure of 0.5 rap means half of room air pressure.

According to Equation 8, we need to know  $\frac{\Delta N}{\Delta P}$  to determine the linear coefficient k. Note that we are interested in changes of pressure rather than the individual values of pressure. Using the data from Table 1, we can obtain the respective  $\Delta P$  and  $\Delta N$  values for each trial. As shown in Figure 5, after

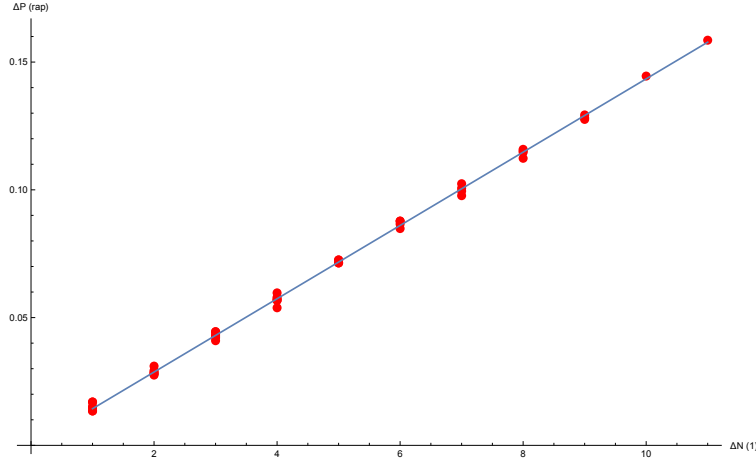


Figure 5:  $\Delta P$  vs.  $\Delta N$  for air in the gas chamber at constructive interferences

graphing all the  $\Delta P$  vs.  $\Delta N$  data points and using a line  $\Delta P = a\Delta N$  to fit these points, we can obtain  $\frac{\Delta P}{\Delta N} = a = 0.0143445$  with Mathematica. Therefore, from Equation 8, we can obtain the linear coefficient for air  $k = \left(\frac{\lambda_0}{2l}\right)\left(\frac{\Delta N}{\Delta P}\right) = \frac{632.991nm}{2 \times 100mm} \times \frac{1}{0.0143445} = 0.000220639$ , where the wavelength of HeNe laser in vacuum of 632.991nm is used.<sup>9</sup> Notice that this value of k has a unit of  $rap^{-1}$ . Use the outdoor air pressure as an approximation for the room air pressure, we have  $1rap = 1.0103atm$ . Therefore,  $k = 0.00021839atm^{-1}$ . As



per Equation 2, we can determine the index of refraction of air at 1atm and 23 °C (the room temperature) to be 1.0002184. Using the refractive index of air calculator provided by National Institute of Standards and Technology (NIST),<sup>10</sup> I calculated the index of refraction of air at the laboratory condition to be around 1.00027, corresponding to a linear coefficient  $k$  of  $0.00027\text{atm}^{-1}$ . Therefore, the experimentally determined linear coefficient is less than the expected result by about 19 percent.

#### 4.2.2 Index of refraction of helium

As mentioned in Section 3.3.2, to determine the index of refraction of helium at room temperature, 2 groups of trials were carried out. Helium gas was expected to flow into the gas chamber more slowly in the first group of trials than the second group because the gas inlet valve was opened to a smaller extent in the first group of trials.

**Group 1** The first group consists of 6 trials. Each trial has a data recording period of 5 seconds and a recording frequency of 1000 times per second. The gas chamber helium pressures and the respective times of constructive interference are presented in Table 2. The  $\Delta P$  vs.  $\Delta N$  plot, with a fitting line, for all the data points in Table 2 is displayed in Figure 6. The fitting result, obtained with Mathematica, is

Helium Trial 1 (Group 1)		Helium Trial 2 (Group 1)		Helium Trial 3 (Group 1)	
time(s)	pressure(rap)	time(s)	pressure(rap)	time(s)	pressure(rap)
0.75	0.45639305	0.75	0.347561414	1.05	0.084841222
2.15	0.505548232	2.15	0.404325944	3.05	0.131659676
3.75	0.557627322	3.65	0.461665668		
Helium Trial 4 (Group 1)		Helium Trial 5 (Group 1)		Helium Trial 6 (Group 1)	
time(s)	pressure(rap)	time(s)	pressure(rap)	time(s)	pressure(rap)
0.35	0.193097663	0.75	0.289047334	0.75	0.19777112
1.05	0.216500899	2.25	0.333517076	2.25	0.245751947
2.25	0.25453565	3.85	0.378573996	3.75	0.290808868
3.65	0.297831037				

Table 2: Group 1: gas chamber helium pressures at times of constructive interference. The unit, rap, means room air pressure.

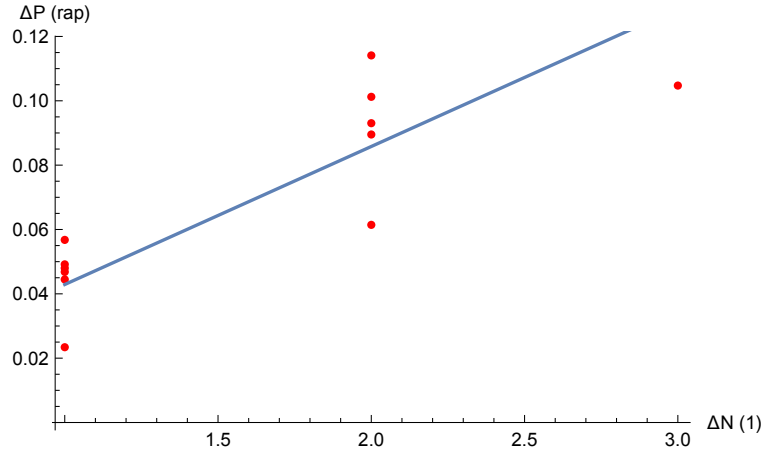


Figure 6: Group 1:  $\Delta P$  vs.  $\Delta N$  for helium in the gas chamber at constructive interferences

$\Delta P = 0.0428993\Delta N$ . Following the same procedure as we did for air, we obtained the linear coefficient  $k = 0.00007302\text{atm}^{-1}$ . This indicates an index of refraction of helium at 1atm and 23 °C to be 1.00007302.

**Group 2** The second group consists of 4 trials. The first trial has a data recording period of 5 seconds while the other 3 trials has that of 10 seconds. The recording frequency was kept at 1000 times per second.

The experimental data and the corresponding fitting plot, like for Group 1, are presented in Table 3 and Figure 7. As shown in Figure 7, the fitting line found by Mathematica is  $\Delta P = 0.066651\Delta N$ . Following

Helium Trial 1 (Group 2)		Helium Trial 2 (Group 2)		Helium Trial 3 (Group 2)		Helium Trial 4 (Group 2)	
time(s)	pressure(rap)	time(s)	pressure(rap)	time(s)	pressure(rap)	time(s)	pressure(rap)
0.55	0.269155183	1.15	0.073145596	2.05	0.081342121	3.05	0.084841222
1.05	0.331767525	1.65	0.142768125	2.55	0.152726183	3.45	0.140431396
1.75	0.414859197	2.15	0.21122828	2.95	0.208304374	3.95	0.208304374
2.35	0.479796285	2.55	0.263894548	3.45	0.275590174	4.35	0.261557819
3.15	0.55996405	3.05	0.327669263	3.85	0.327082085	4.85	0.324158179
3.95	0.629586579	3.65	0.400227681	4.45	0.401390054	5.45	0.396129419
4.85	0.69747154	4.25	0.467513481	5.05	0.46985021	6.05	0.463415219
		4.95	0.539484721	5.75	0.543582984	6.75	0.535386459
		5.75	0.613205512	6.45	0.609694428	7.45	0.60033553
		6.55	0.677567406	7.35	0.683427202	8.35	0.672893948
		7.75	0.756560815	8.35	0.752462552	9.55	0.752462552
		9.25	0.831455962	9.85	0.830293589		

Table 3: Group 2: gas chamber helium pressures at times of constructive interference. The unit, rap, means room air pressure.

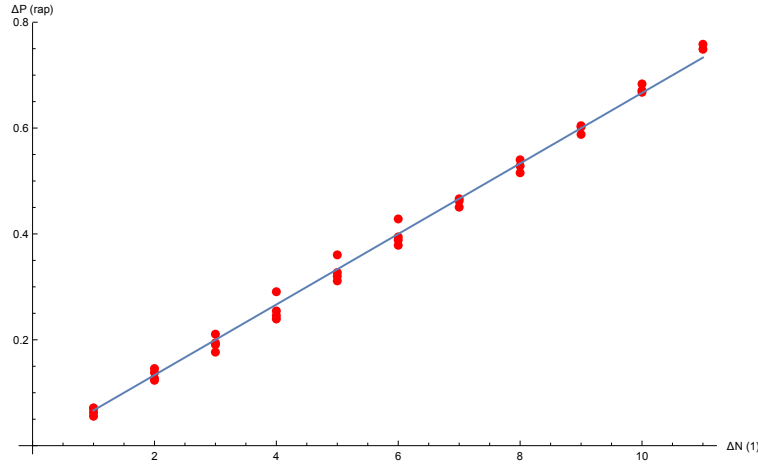


Figure 7: Group 2:  $\Delta P$  vs.  $\Delta N$  for helium in the gas chamber at constructive interferences

the same procedure as we did for air, we obtained the linear coefficient  $k = 0.00004700 \text{ atm}^{-1}$ . This indicates an index of refraction of helium at 1atm and 23 °C to be 1.00004700.

As we can see, the linear coefficient obtained from the first group of trials ( $0.00007302 \text{ atm}^{-1}$ ) is larger than that obtained from the second group of trials ( $0.00004700 \text{ atm}^{-1}$ ) by about one half. In fact, as we can see from Table 4 and Table 5, the 6 trials of experiments in Group 1 show a distinct  $\Delta P$  vs.  $\Delta N$  pattern from that of Group 2. Both Table 4 and Table 5 document the changes of gas chamber helium pressure between successive constructive interferences. For Group 1 where I opened the gas inlet valve to a smaller extent, the consecutive pressure changes for each trial are clearly around 0.045rap, while those for the Group 2 trials are clearly around 0.07rap. Therefore, the results from Group 1 and Group 2 are consistent within each group, but are not very consistent between the two groups. The expected index of refraction of helium, at the laboratory condition, is 1.000035.<sup>11</sup> So, considering the linear coefficient k for helium, the result from Group 2 is about 34 percent larger than the expected value, while that from Group 1 is about 2 times larger than the expected value.

$\Delta N$	$\Delta P$ (rap)	$\Delta N$	$\Delta P$ (rap)	$\Delta N$	$\Delta P$ (rap)
Trial 1		Trial 2		Trial 3	
1	0.049155183	1	0.05676453	1	0.046818454
1	0.052079089	1	0.057339724		
Trial 4		Trial 5		Trial 6	
1	0.023403235	1	0.044469742	1	0.047980827
1	0.038034751	1	0.04505692	1	0.04505692
1	0.043295386				

Table 4: Group 1: Gas chamber helium pressure increments at constructive interferences.

Trial 1		Trial 2		Trial 3		Trial 4	
$\Delta N$	$\Delta P$ (rap)	$\Delta N$	$\Delta P$ (rap)	$\Delta N$	$\Delta P$ (rap)	$\Delta N$	$\Delta P$ (rap)
1	0.062612343	1	0.069622528	1	0.071384062	1	0.055590174
1	0.083091672	1	0.068460156	1	0.055578191	1	0.067872978
1	0.064937088	1	0.052666267	1	0.0672858	1	0.053253445
1	0.080167765	1	0.063774715	1	0.051491911	1	0.062600359
1	0.069622528	1	0.072558418	1	0.074307969	1	0.07197124
1	0.067884961	1	0.0672858	1	0.068460156	1	0.0672858
		1	0.07197124	1	0.073732774	1	0.07197124
		1	0.073720791	1	0.066111444	1	0.064949071
		1	0.064361893	1	0.073732774	1	0.072558418
		1	0.078993409	1	0.069035351	1	0.079568604
		1	0.074895147	1	0.077831037		

Table 5: Group 2: Gas chamber helium pressure increments at constructive interferences.

## 5 Conclusion

This experiment was intended to measure the wavelength of HeNe laser and the indices of refraction (or linear coefficients  $k$ ) of air and helium at normal room conditions.

**Wavelength of HeNe laser** The wavelength of HeNe laser at the laboratory condition was measured to be 683.0nm, which is larger than the expected result (632.8nm) by about 8 percent. Therefore, the expected result is smaller than the experimental result by 7.3 percent. According to Equation 4, this means that the measured time intervals between successive constructive interferences are, on average, larger than the expected time intervals, or the displacement speed of the right reflector mirror taken into the calculation was larger than the true value, or there were inaccuracies in both places. First, the displacement speed used in the calculation was not likely to contribute much to the 7.3 percent error, because the speed of revolution of the driving motor was carefully verified to be 1 revolution per minute by observing the position of the micrometer's graduation after every minute of rotation for 7 minutes. Using the graduation on the micrometer, I have confidence in constraining the uncertainty of the used rotation speed of the micrometer to within 0.13 percent. Given the possible uncertainties from the calibration of the micrometer, I do not see a good likelihood for the used displacement speed of the right reflector mirror to have an uncertainty over 0.25 percent. So, the major source of error should come from the measured time intervals between successive constructive interferences. As shown in Figure 4, these time intervals do fluctuate quite a bit, although in theory they should be nearly identical given the nearly constant rotation speed of the motor. One cause for the measured time interval fluctuations might come from the methodology of obtaining the times at constructive interferences. These critical times were located with a computer program that compared the total intensities between successive groups of consecutive times. In this investigation, 24 consecutive recorded times (0.024s) were used as a group and the times for constructive interference were taken from the mid-point times in the groups that have locally maximum total intensities. The reason that I adopted this time-grouping methodology is that there is no absolute point of time of a locally maximum intensity due to inherent fluctuations of the detected intensities. Therefore, there is an inherent 0.024s uncertainty for the calculated average time interval of 0.409788s obtained in Section 4.1, corresponding to a uncertainty of  $\pm 5.9$  percent. This uncertainty is smaller than the actual -7.3 percent error. So, the -7.3 percent error

might also come from the measurement of the interfering light intensity. Using 0.409788s as the average (notice that it is a linear fitting average rather than an arithmetic mean), the standard deviation for the measured time intervals in Figure 4 is calculated to be 0.09186s. So, the uncertainty from the standard deviation is  $\pm 22.4$  percent. Therefore, the experimental error of 7.3 percent lies well within this range. This uncertainty of 22.4 percent might come from inaccuracies of measurements with the photodetector or the aforementioned methodology to pinpoint peak intensities. The inaccuracies of the measurements might be owing to slight vibrations of the optical devices caused by the kept-running vacuum pump on the floor. Slight vibration of the optical devices would cause the interfering light on the photodetector to vibrate slightly, which might negatively influence the accuracy of the measured light intensity. To improve the accuracy of the experimental results, the vacuum pump could be turned off before the computer interface started to record the experimental data.

**Index of refraction of air** The linear coefficient  $k$  for air in the  $n = kP + 1$  relationship was measured to be  $0.0002184\text{atm}^{-1}$  under the laboratory condition. This is less than the expected result ( $0.00027\text{atm}^{-1}$ ) by 19 percent. Therefore, the expected result is larger than the experimental result by 23.6 percent. According to Equation 8, this means that for the horizontally-split laser beam to travel an additional wavelength, the measured changes of gas chamber air pressure  $\Delta P$  are, on average, larger than the expected change of gas chamber air pressure. As discussed in the previous paragraph, the times for constructive interferences would be pinpointed with uncertainties due to the methodology to extract the peak intensities. For the 6 trials in this investigation, time-grouping intervals between 0.05s and 0.1s were used in the computer program to locate times of constructive interference, because the regions corresponding to a constructive interference display a more flattened-out intensity as shown in Figure 8. So, for each trial, I calculated the

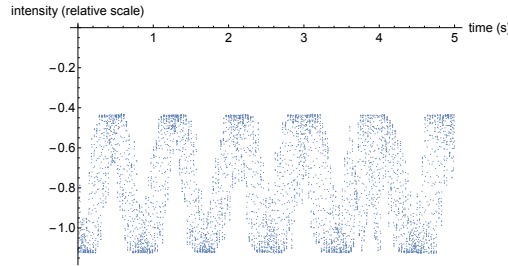


Figure 8: A sample graph for the measured intensities in the investigation of air's refractive index (Trial 6)

standard deviation of the measured pressures in each identified time-group corresponding to a constructive interference. I averaged these standard deviations for each trial, and then I took an average again of these averaged standard deviations for all 6 trials. Finally, I got an average standard deviation of the measured pressures in all the critical time-groups to be  $0.0005813\text{rap}$ . Since we are interested in the changes of pressure between successive constructive interferences, the change of pressure between two successive critical pressures has an uncertainty of approximately  $\pm 0.0005813\text{rap} \times 2 = \pm 0.001163\text{rap}$ , since I chose the mid-point pressure in each time-group as the critical pressure. Recall from Section 4.2.1, we obtained an average  $\frac{\Delta P}{\Delta N}$  by linear line fitting to be  $0.0143445\text{rap}$ . So the uncertainty in the calculated  $\frac{\Delta P}{\Delta N}$  value is  $\pm \frac{0.001163}{0.0143445} = \pm 8.1\text{percent}$ . Notice that the linear coefficient  $k$  is inversely proportional to  $\frac{\Delta P}{\Delta N}$ , so the corresponding uncertainty for  $k$  is  $+8.8$  percent and  $-7.5$  percent, from the inherent uncertainty in identifying the critical intensities from the experimental data. This uncertainty range does not cover the actual error of  $+23.6$  percent. Another source of error might come from the measured values of air pressure at the times of constructive interference, since there is an inherent uncertainty about measurements with the pressure sensor. Theoretically, for the linear coefficient  $k$  to be constant, the change of pressure  $\Delta P$  over 2 successive times of constructive interference should also be a constant. So, I calculated the standard deviation of such  $\Delta P$  from experimental data of all 6 trials in Table 1, using the average  $\Delta P$  value of  $0.0143445\text{rap}$  obtained from the linear line fitting process in Section 4.2.1. This standard deviation of  $\Delta P$  was found to be  $0.001247\text{rap}$ , corresponding to an uncertainty of  $+9.4$  percent or  $-7.9$  percent for the linear coefficient  $k$ . Notice that this uncertainty is partly due to the aforementioned uncertainty in locating peak intensities, so I can only take the union between the  $\langle -7.5 \text{ percent}, +8.8 \text{ percent} \rangle$  uncertainty range and the  $\langle -7.9 \text{ percent}, +9.4 \text{ percent} \rangle$  uncertainty range rather

than simply add up these two ranges. The union uncertainty range, which is  $\langle -7.9 \text{ percent}, +9.4 \text{ percent} \rangle$ , does not account for the 23.6 percent error well, so uncertainties of the experimental result should come from additional places. Notice that we assume temperature of the air in the gas chamber remained the same as that of the room temperature. This would not be so in reality, since as air flowed into the gas chamber, which was initially in vacuum, air would do positive work and thus its temperature would decrease. In this case, we no longer have a constant linear coefficient  $k$  according to Section 2 and thus our experimental result might be affected by this fact. To partially verify this hypothesis, more trials of experiments could be conducted to see whether the experimentally determined linear coefficient kept remaining smaller than the expected result and careful theoretical analyses on the thermodynamics of the air flowing into the gas chamber could be performed to check against the experimental results.

**Index of refraction of helium** In the investigation of helium's refractive index, two groups of trials were conducted. The first group found the linear coefficient  $k$  for helium at the laboratory conditions to be  $0.00007302 \text{ atm}^{-1}$ , while the second group found that to be  $0.00004700 \text{ atm}^{-1}$ . The result from Group 1 is twice larger than the expected result ( $0.000035 \text{ atm}^{-1}$ ), while that from Group 2 is larger than the expected result by 34 percent. Therefore, the expected result is less than the experimental result from Group 1 by about 50 percent, and less than that from Group 2 by 25.5 percent. Using the same error analysis techniques that I used for analyzing the linear coefficient of air, for Group 1 the uncertainty due to the time-grouping methodology is around  $\pm 4.3$  percent, and for Group 2 that is around  $\pm 9.3$  percent. Also, for Group 1, the uncertainty due to the standard deviation of the successive  $\Delta P$  values is  $+26.7$  percent and  $-17.4$  percent. For Group 2, this uncertainty is  $+13.6$  percent and  $-10.7$  percent. For each group, the lower-bound of the uncertainty ( $-10.7$  percent and  $-17.4$  percent, respectively) does not cover the actual experimental error. Notice that the experimentally-determined indices of refraction of helium is higher than the expected value, and air does have an index of refraction (1.00027) higher than that of helium (1.000035) at the laboratory conditions. Therefore, the high linear coefficients of helium determined from the experiment might be in part due to air mixed in the bag of helium. This is possible since air was likely to leak into the helium bag when I was trying to seal the opening of the helium bag to the outer open end of the syringe. Even after the helium bag was sealed to the syringe, the remaining air in the gas inlet pipe (in the region between the gas inlet valve and the outer end of the syringe) would inevitably mix into the helium bag. Moreover, there might also be air mixing with helium during the preparation of the helium bag. Since the linear coefficient for air is almost 8 times larger than that of helium, the pollution of helium by air is likely to be influential in the deviation of the experimentally determined result from the expected result, and thus the experimental error of the linear coefficient of helium is explainable. However, as discussed in Section 4.2.2, the experimental results are consistent within each group but are not so across the groups. The measured changes of pressure when the helium gas flowed into the gas chamber more slowly are evidently smaller than those when the helium gas flowed into the gas chamber faster. Since the helium temperature would not be constant during the process, this difference might be due to the different rates of change of the thermodynamics of the helium, but the precise mechanism needs more careful thermodynamics analyses. To investigate the cause more carefully, more trials could be done at different extents of opening of the gas inlet valve to compare the experimental results. In general, to improve the accuracy of the experimentally determined linear coefficient of helium, relevant procedures should be taken to prevent air from leaking into the helium bag.

## References

- <sup>1</sup>J. Cutnell and K. Johnson, *Physics*, 9th ed. (Wiley, Hoboken, NJ, 2012), pp. 838–841.
- <sup>2</sup>B. H. Bunch and A. Hellemans, *The history of science and technology: a browser's guide to the great discoveries, inventions, and the people who made them, from the dawn of time to today* (Houghton Mifflin Harcourt, New York, 2004).
- <sup>3</sup>D. Huang et al., *Science* (New York, NY) **254**, 1178 (1991).
- <sup>4</sup>A. Curtis, P. Gerstoft, H. Sato, R. Snieder, and K. Wapenaar, *The Leading Edge* **25**, 1082–1092 (2006).
- <sup>5</sup>B. P. Abbott et al., *Phys. Rev. Lett.* **116**, 241103 (2016).
- <sup>6</sup>J. Cutnell and K. Johnson, *Physics*, 9th ed. (Wiley, Hoboken, NJ, 2012), pp. 836–837.

- <sup>7</sup>J. Cutnell and K. Johnson, *Physics*, 9th ed. (Wiley, Hoboken, NJ, 2012), pp. 846–850.
- <sup>8</sup>D. Griffiths, *Introduction to electrodynamics*, 4th ed. (Pearson Education, Glenview, IL, 2014), pp. 417–424.
- <sup>9</sup>A. Saha and N. Manna, *Optoelectronics and optical communication* (Laxmi Publications Pvt Limited, New Delhi, India, 2011), p. 101.
- <sup>10</sup>J. A. Stone Jr and J. H. Zimmerman, *Refractive index of air calculator based on modified edlén equation*, (2001) <http://emtoolbox.nist.gov/Wavelength/Edlen.asp>.
- <sup>11</sup>M. Polyanskiy, *Optical constants of helium*, (2008) <https://refractiveindex.info/?shelf=main&book=He&page=Mansfield>.